Journal Pre-proofs

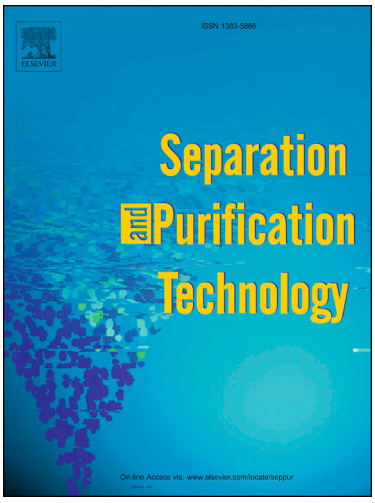

CO_2 removal from anaesthesia circuits using gas-ionic liquid membrane contactors

C.F. Martins, L.A. Neves, R. Chagas, L.M. Ferreira, C.A.M. Afonso, J.G. Crespo, I.M. Coelhoso

PII: S1383-5866(20)31457-X
DOI: https://doi.org/10.1016/j.seppur.2020.116983
Reference: SEPPUR 116983

To appear in: *Separation and Purification Technology*

Received Date: 16 November 2019
Revised Date: 25 March 2020
Accepted Date: 27 March 2020

Please cite this article as: C.F. Martins, L.A. Neves, R. Chagas, L.M. Ferreira, C.A.M. Afonso, J.G. Crespo, I.M. Coelhoso, CO_2 removal from anaesthesia circuits using gas-ionic liquid membrane contactors, *Separation and Purification Technology* (2020), doi: https://doi.org/10.1016/j.seppur.2020.116983

CO_2 removal from anaesthesia circuits using gas-ionic liquid membrane contactors

C. F. Martins[a], L. A. Neves[a], R. Chagas[b], L. M. Ferreira[a], C. A. M. Afonso[c], J. G. Crespo[a], I. M. Coelhoso[a,*]

[a] *LAQV/Requimte, Departamento de Química, Faculdade de Ciências e Tecnologia, Universidade NOVA de Lisboa, 2829-516 Caparica, Portugal.*

[b] *i3N/CENIMAT Department of Materials Science, Faculdade de Ciências e Tecnologia, Universidade NOVA de Lisboa Campus de Caparica, 2829-516 Caparica, Portugal*

[c] *Research Institute for Medicines (iMed.ULisboa), Faculty of Pharmacy, Universidade de Lisboa, Av. Prof. Gama Pinto, 1649-003 Lisboa, Portugal.*

[*] *Corresponding author: imrc@fct.unl.pt*

Abstract

Nowadays, the reutilization of anaesthetic gases is accomplished by capturing carbon dioxide with soda lime, a solid adsorbent mostly composed by calcium and sodium hydroxide. To overcome the issues regarding the use of soda lime, this work proposes an alternative process to remove carbon dioxide through the use of a membrane contactor combined with a biocompatible ionic liquid (IL), cholinium lysinate, with high absorption capacity (5.9 mol_{CO2}/kg_{IL}). The carbon dioxide removal rate and IL solution regeneration, were assessed, varying the feed gas composition, relative humidity and ionic liquid flow rate conditions. Overall mass transfer coefficients and separation factors were determined. From the results obtained, the proposed system is feasible to remove carbon dioxide from anaesthetic gas circuits. Moreover, the system working operation time obtained was 63 hours, which in a mass basis comparison with soda lime (current technology), is 3 to 5 times higher.

Keywords: CO_2 removal, biocompatible ionic liquid, gas-liquid membrane contactor, anaesthetic gas.

1. Introduction

In the conventional technology to remove carbon dioxide (CO_2) from inhalation anaesthesia circuits, a container with soda lime is used to adsorb and degrade the expired gases and anaesthetics [1]. Soda lime is composed mostly by calcium and sodium hydroxide, which is proved to remove CO_2 efficiently [2]. Furthermore, it is used in anaesthetic circuits in a closed-loop operating mode, where the expired CO_2 is removed to allow the recovering and recycling of the non-absorbed anaesthetics. Typically, the inhaled anaesthetic gas mixture is composed by 70% of the anaesthetic gas and 30% of oxygen, which results in an exhaled gas mixture with 65% of anaesthetic gas, 27% of oxygen, 5% of carbon dioxide and 3% of nitrogen. The reuse of the non-absorbed anaesthetics is only possible if the carbon dioxide concentration is lowered down to 0.5% [3,4].

Even though soda lime is used in these circuits, efforts must be done to replace the current technology, due to existent drawbacks. Several studies show that volatile halogenated hydrocarbons typically present in anaesthetic streams (e.g. sevoflurane, desflurane and isoflurane) can react with soda lime with low water content, being chemically degraded to vinyl-ether molecules known as compounds A–E [1,5]. These compounds along with other toxic compounds, such as carbon monoxide, may present potential life-threatening complications [6,7].

The most used technique for CO_2 capture (from diverse gas streams sources) is absorption using aqueous amine solutions, specially solutions containing monoethanolamine (MEA) [8]. This technique consists in scrubbing CO_2 from a gas mixture with the aqueous amine solution in a packed column, followed by a liquid regeneration step with stripping water vapour at temperatures between 373 and 393 K [9]. However, drawbacks including corrosion, oxidative degradation, negative environmental impact, high volatility leading to considerable losses of the absorbent, chemical and thermal instabilities and low energy efficiency, motivate researchers to seek for more efficient and environment-friendly alternatives [8,10–12].

Studies on CO_2 capture using different absorption systems increased progressively over the last three decades, where ionic liquids (ILs) are emerging as a potential alternative [13]. ILs are liquid salts with negligible volatility and their potential to capture CO_2 is recognized due to their unique properties, such as the ability to be tuned for each specific process, excellent thermal stability, structural functionality, among others. Furthermore, ILs are able to work as solvents and also for this reason their potential is being explored to replace conventional CO_2 absorbents [14]. CO_2 capture and conversion studies using amino-acid based ILs combined with the cholinium cation, revealed their strong ability to react with CO_2, are more resistant to oxidative degradation and exhibit a higher thermal stability [4,15–19]. Additionally, this group of ILs is even more interesting due to their low toxicity, biocompatibility and biodegradability. Bhattacharyya *et al.* [17] synthesized novel ILs containing choline ([Cho]) based on ether functionalized cations with amino acid ([AA]) anions, aiming an effective CO_2 capture performance and stability in the presence of oxygen. The synthesized $[N_{1,1,6,2O4}]$[Lys] IL presented a CO_2 capture capacity of 4.31 mol_{CO2}/kg_{IL} (at 293 K). Li *et al.* [15] studied the absorption of CO_2 in 30 wt% aqueous solutions of [Cho][AA]s ILs, obtaining a CO_2 capture capacity of 0.89 mol_{CO2}/kg_{IL} for the cholinium lysinate ([Cho][Lys]) IL, at 303 K and close to the atmospheric pressure. Li *et al.* proposed the use of aqueous solutions of this family of ILs, in order to reduce the viscosity, the gas-liquid mass transfer resistance, as well as to turn the ILs more economically viable for the CO_2 capture application, when compared to less expensive solutions such as aqueous amines.

The use of porous membrane contactors for CO_2 capture using ionic liquids or amino acid salt solutions, as liquid absorbents has also been addressed [20–23]. In this approach, a porous hydrophobic membrane is used to promote the contact between gas and liquid phases, without dispersion of one phase into the other. Furthermore, the hydrophobic character of the membrane prevents the liquid from entering the pores, minimizing the mass transfer resistance of the membrane. Thus, the membrane acts as a separation barrier providing interfacial area for mass transfer, while the selectivity is given by affinity to the liquid phase [20, 24]. Portugal *et al.* [4] proposed this approach for the CO_2 removal from anaesthetic gas circuits, using potassium

glycinate solutions, as the liquid absorbent, and hollow fiber contactors with a composite membrane made of a porous support of polyethylenimine (PEI) and a polydimethylsiloxane (PDMS) dense thin layer. For the same purpose, Sirkar *et al.* [25] proposed the use of hydrophilic porous hollow fiber membrane contactors, with glycinate/glycerol solutions impregnated inside the pores. Another alternative process was presented by Malankowska *et al.* [26] using a microfluidic gas-ionic liquid contactor, with a cholinium propionate solution containing the carbonic anhydrase enzyme, for CO_2 enhanced transport, to remove CO_2 from anaesthetic circuits with xenon.

Following this concept, the present work discusses the removal of CO_2 from a closed-loop system containing complex gas mixtures with anaesthetic agents, using a membrane contactor comprised of porous capillaries of polytetrafluoroethylene (PTFE) and a cholinium lysinate ionic liquid solution as a biocompatible and cost-effective CO_2 absorbent. The IL solution contains 50 wt% of water, to minimize operation constraints (i.e. overpressure inside the capillaries due to the high viscosity), as well as to minimize the cost when comparing to the operation with an IL with higher purity. Regarding the porous membrane selected, it is recognized that PTFE possesses high chemical resistance and retain their non wetting behaviour even in the presence of corrosive chemicals [27]. For this reason, Eclipse™ membranes were selected for the present study. To validate the concept proposed, the following aspects were investigated: 1) Total CO_2 capture capacity of the system; 2) CO_2 capture capacity, with humidified and dried simulated exhaled N_2O streams, with low CO_2 partial pressures; 3) IL solution regeneration efficiency using a sweep gas. The overall mass transfer coefficient and the CO_2/N_2O separation factor (SF) were also evaluated and the proposed technology for CO_2 removal was compared with the present technology using soda lime.

2. Theory

2.1. CO_2 absorption with chemical reaction

[Cho][Lys] is an IL derived from the cholinium family with the amino acid lysine as anion. Despite the existence of physical diffusion of CO_2 in this IL, the dominant phenomenon of transport is attributed to the chemical reaction between the IL and CO_2 [28]. [Lys] anion is an amphoteric species which, combined with the [Cho] cation, acts as a Lewis acid due to the presence of the ammonium group in the cation. In the presence of water, the [Lys] anion with its two amino groups acts as a strong base and CO_2 absorption occurs *via* bicarbonate and carbonate formation [28]. The contact between the amino groups and bicarbonate is extremely reactive. The following simplified model describes the CO_2 absorption by chemical reaction in this IL:

$$H_2O \overset{K_1}{\leftrightarrow} H^+ + OH^- \quad (1)$$

$$CO_2\,(aq) + OH^- \overset{K_2}{\leftrightarrow} HCO_3^- \quad (2)$$

$$[Cho][Lys] + HCO_3^- \overset{K_3}{\leftrightarrow} CO_3^{2-} + [Cho][Lys]H^+ \quad (3)$$

$$[Cho][Lys] + H^+ \overset{K_4}{\leftrightarrow} [Cho][Lys]H^+ \quad (4)$$

$$[Cho][Lys]H^+ + HCO_3^- \overset{K_5}{\leftrightarrow} [Cho][Lys]H^+ HCO_3^- \quad (5)$$

In the described mechanism, all species are involved in reversible reactions. However, it is important to mention that regarding equation (2), $CO_2\,(aq)$ concentration is always null, due to the fast conversion into bicarbonate, HCO_3^- and carbonate, CO_3^{2-} (depending on the pH).

2.2. CO_2 mass transfer models

In this work, the gas phase flows counter-currently with the liquid phase, promoting a maximum driving force between the phases along the membrane contactor. Furthermore, the high hydrophobic character of the PTFE membrane allows for operation in a non-wetted pore mode, avoiding the resistance promoted in the case of stagnant liquid inside the pores, as it is depicted in Figure 1 [24].

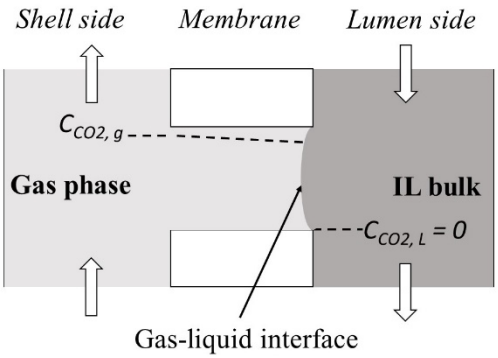

126

127 *Figure 1. CO_2 mass transfer in a non-wetted pore mode.*

128 CO_2 mass transfer from the gas to the liquid phase includes diffusion from the gas stream
129 through the membrane pores and diffusion in the liquid phase, which in this work, is accompanied
130 by a fast chemical reaction. The CO_2 flux (J_{CO2}, in mol.m^{-2}.s^{-1}), from the gas to the liquid phase
131 is described by:

132 $$J_{CO2} = K_{ov} \times (CO_2 - CO_2^*) \qquad (6)$$

133 where $(CO_2 - CO_2^*)$ is the concentration driving force (mol.m^{-3}), CO_2 is the carbon dioxide
134 concentration in the gas phase, CO_2^* is the carbon dioxide concentration in equilibrium with the
135 concentration of CO_2 in the liquid phase, being null in this case, since $CO_{2\,IL} = 0$. K_{ov} is the overall
136 mass transfer coefficient (m.s^{-1}), which is obtained by the resistance-in-series approach [29].

137

138 $$\frac{1}{K_{ov}} = \underbrace{\frac{1}{k_g}}_{\text{gas phase resistance}} + \underbrace{\frac{d_0}{k_m \times d_{lm}}}_{\text{membrane resistance}} + \underbrace{\frac{d_0}{\varphi \times d_i \times k_l}}_{\text{liquid phase resistance}} \qquad (7)$$

139

140 where φ is the product between the gas-liquid partition coefficient -m- and an enhancement factor
141 -E- due to the chemical reaction contribution in the CO_2 absorption, d_0, d_{lm} and d_i are the external,
142 logarithm mean and internal diameters of the capillaries, k_g, k_m and k_l are the individual mass
143 transfer coefficients in the gas, membrane and liquid. In a non-wetted pore operation mode, mass
144 transfer resistances in the gas phase (k_g^{-1}) and membrane ($d_0.d_{lm}^{-1}.k_m^{-1}$) are negligible, and the
145 liquid phase resistance controls the CO_2 mass transfer in the module. In this work, the liquid phase

flows in laminar regime inside the capillaries of the Eclipse™ module (Reynolds number, ≤ 2200). Therefore, the liquid mass transfer coefficient (k_l, in m.s^{-1}) can be estimated using the following equation [29,30]:

$$\frac{k_l \times d_i}{D_{CO2,\ l}} = 1.62 \times \left(\frac{d_i^2 \times u_l}{L \times D_{CO2,\ l}}\right)^{0.33} \quad (8)$$

where d_i is the capillaries internal diameter (m), $D_{CO2,\ l}$ the CO_2 diffusion coefficient in the liquid (m^2.s^{-1}), u_l the average liquid velocity (m.s^{-1}) and L the capillaries length (m). In a previous work, it was reported a predictive correlation between CO_2 diffusion coefficient and viscosity for cholinium-based ILs [19]. To estimate the CO_2 diffusion coefficient in [Cho][Lys], the following assumptions were considered: the absorption capacity of the ionic liquid is dependent on the anion nature; the experiments must be performed under isothermal conditions; and the viscosity of the ionic liquid does not vary with the absorption of the gas. CO_2 diffusion coefficient in the IL [Cho][Lys] can be obtained through the following equation:

$$D_{CO2,\ l} = 6.569 \times 10^{-6} \frac{\mu^{-0.805 \pm 0.087} \times V_{m,\ IL}^{0.508 \pm 0.009}}{\rho^{0.507 \pm 0.006}} \quad (9)$$

where μ is expressed in Pa.s, $V_{m,IL}$ in m^3.mol^{-1} and ρ in kg.m^{-3} are the ionic liquid viscosity, molar volume and density, respectively.

3. Experimental

3.1. Materials

The [Cho][Lys] ionic liquid was synthesized from a choline hydroxide solution (45 wt% in methanol, Acros Organics, USA) and L(+)-Lysine monohydrate (99%, Acros Organics, USA), supplied by Thermofisher Scientific. The gases used in the experiments were carbon dioxide (CO_2, high-purity grade 99.998%, Praxair, USA), oxygen (O_2, purity grade 99.999%, Praxair, USA), nitrogen (N_2, purity grade 99.998%, Praxair, USA), nitrous oxide (N_2O, purity grade 99.6%, Air Liquide, France) and helium (He, purity grade 99.998%, Praxair). Two identical gas-liquid membrane contactors were used for the CO_2 capture and IL solution isothermal regeneration. Membrane modules are composed by Eclipse™ capillary membranes, supplied by

171 Markel Corporation (USA) and are made of porous polytetrafluoroethylene, assembled in a
172 stainless-steel housing. Membrane and module specifications were provided by the supplier and
173 are presented in Table 1.

174 *Table 1. Eclipse™ membrane modules specifications.*

Capillaries		**Modules**	
Inner diameter (mm)	1.5	*Number of fibers (N)*	537
Outer diameter (mm)	1.9	*Active area (m^2)*	1
Porosity (%)	53	*Inner diameter (mm)*	60
Maximum pore diameter (µm)	0.82	*Effective length (mm)*	406
Mean pore diameter (µm)	0.65		
Minimum pore diameter (µm)	0.61		

175

176 *3.2. [Cho][Lys] synthesis and characterization*

177 L(+)-Lysine monohydrate was dissolved in water and added directly to choline hydroxide *via* a
178 neutralization reaction. The final product was an aqueous solution of [Cho][Lys] ionic liquid,
179 containing 50 ± 2% (w/w) of water. No dehydration step was performed in the IL solution. The
180 reaction was followed by pH measurement, using a Mettler Toledo pH probe (model l405-DPAS-
181 SC-K8S, USA) connected to an in-line tester (Jenco, model 3621, USA). The water content was
182 measured by titration, using a Karl-Fischer coulometer without diaphragm (Metrohm, USA,
183 model 831 KF coulometer). The [Cho][Lys] molecular structure was confirmed by proton nuclear
184 magnetic resonance (^{1}H-NMR) and by attenuated total reflectance Fourier transform infra-red
185 (ATR-FTIR) analyses. Both spectra were recorded at room temperature on a Bruker AVANCE
186 Digital operating at 400 MHz and a Perkin Elmer Spectrum Two FT-IR Spectrometer,
187 respectively. [Cho][Lys] thermal stability was accessed by thermogravimetric analysis (TGA),
188 with 10 K per minute up to 873 K under nitrogen environment with a flow rate of 40 mL.min^{-1},
189 using a Q50 thermogravimetric analyser from TA Instruments (USA). [Cho][Lys] viscosity and
190 density were determined using a Stabinger viscometer™ SVM 3000 from Anton Paar (Austria),

191 in the temperature range between 293 to 308 K. The IL surface tension was also measured using
192 a KSV sigma 702 tensiometer from KSV Instruments Ltd. (Finland), at 293 K. A goniometer
193 (KSV Instruments Ltd., Finland) with image analysis software CAM 2008 was used to measure
194 the contact angle between the IL and the surface of the Eclipse™ membrane. The contact angle
195 was calculated as the average between the right and left contact angles.

196 *3.3. CO_2 absorption and IL solution regeneration experimental procedures*

197 Prior the evaluation of CO_2 absorption in the membrane contactor system, the saturation
198 absorption capacity of the [Cho][Lys] IL solution was evaluated. Experiments were carried out in
199 a stainless steel cell, by monitoring the CO_2 pressure decay with time in contact with a small
200 volume of the IL solution, as described in previous works [19,31]. Different concentrations of
201 [Cho][Lys] aqueous solutions were tested, and the saturation absorption capacity was determined
202 for each one.

203 Afterwards, CO_2 absorption and IL solution regeneration were conducted in a gas-liquid
204 membrane contactor system, as represented in Figure 2, at 295±2 K. Mass flow controllers (Alicat
205 Scientific Inc., MC-series, USA), solenoid valves (ASCO®, USA) and pressure gauges
206 (Omega™, USA), controlled the gas flow. Liquid flow was monitored using positive
207 displacement pumps (Micropump®, GJ series, USA) and digital pressure gauges (WIKA, DG-10
208 series, Germany). The IL solution was constantly stirred using a magnetic stirrer plate (Velp
209 Scientifica®, Germany), the pH was measured using a Mettler Toledo pH probe (model l405-
210 DPAS-SC-K8S, USA) connected to an in-line tester (Jenco, model 3621, USA) and the
211 temperature measured with a digital thermometer (Huberlab, Switzerland).

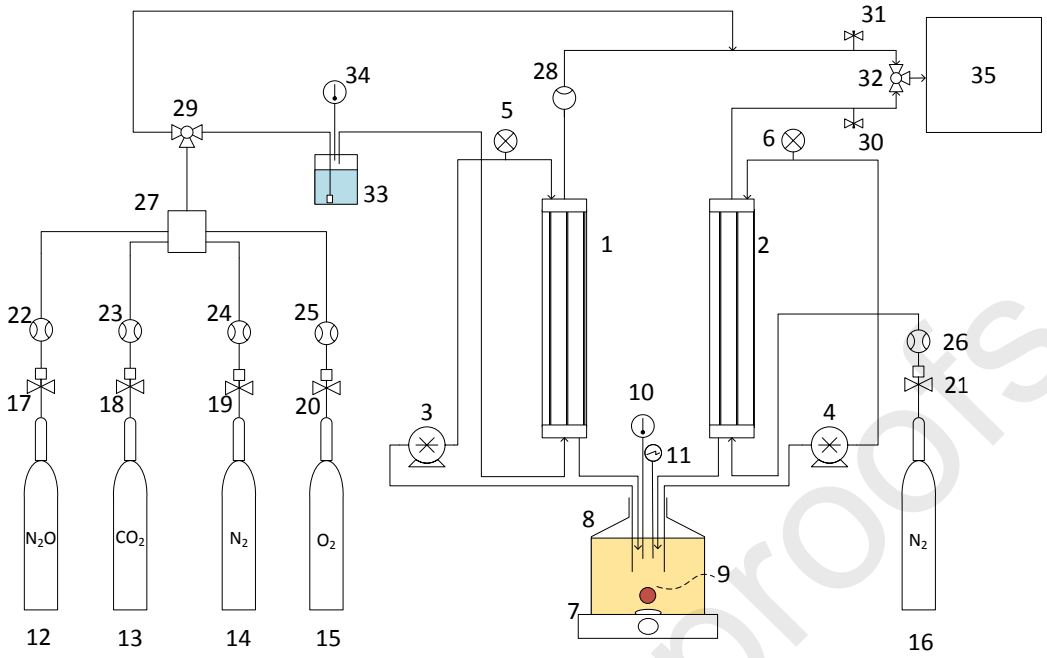

Figure 2. Schematic representation of the experimental set-up: 1, 2 - absorption and regeneration membrane modules, respectively; 3, 4 - positive displacement pumps; 5, 6 - pressure gauges; 7 - stirrer plate; 8 - ionic liquid vessel; 9 - sampling point; 10 - digital thermometer; 11 - pH meter; 12-16 - gas cylinders; 17-21 - solenoid valves; 22-26 - mass flow controllers; 27 - gas mixture unit; 28 - mass flow indicator; 29, 32 - 3 way manual valves; 30, 31 - needle valves, 33 - stainless steel boiler with a gas disperser, 34 – thermocouple, 35 – GC on-line.

Inside the CO_2 absorption module (Figure 2, module 1), the gas phase flowed in the shell side of the contactor, with a constant flow rate of 250 mL.min^{-1}, simulating what is called minimal gas flow rate anaesthesia [32,33]. Since the system was operated in open circuit, the gas pressure was similar to the atmospheric pressure. The IL solution pressure was maintained higher than the gas pressure avoiding bubbling. The [Cho][Lys] solution circulated counter currently, with a constant flow rate of 790 mL.min^{-1}, in the lumen of the capillaries to promote a high driving force between the phases throughout the membrane pores. The regeneration of the IL solution was performed in a second module, connected in series with the absorption module. N_2 at atmospheric pressure with a flow rate of 30 mL.min^{-1} was used as sweep gas. The sweep gas flowed counter currently in the shell side. [Cho][Lys] solution circulated with the lowest flow rate possible (570 mL.min^{-1}), assuring a liquid pressure higher than the sweep gas pressure, in order to avoid bubbling and allow for a higher residence time in the contactor. All the experimental conditions tested are shown in Table 2.

231 *Table 2. Experimental conditions in the absorption and regeneration modules.*

	Absorption module	Regeneration module
Temperature (K)	295±2	
Gas flow rate (mL.min^{-1})	250	30
IL flow rate (mL.min^{-1})	790	570
Feed gas composition (mol%)	3% N_2, 5% CO_2, 27% O_2, 65% N_2O	100% N_2
IL solution inlet pressure (bar)	0.10 - 0.14	0.09
Pressure drop (bar)	0.07	0

232

233 The regeneration efficiency was followed by monitoring the composition of the sweep
234 gas stream at the outlet of the module. Aliquots of IL were collected over time and analysed by
235 ATR-FTIR, to evaluate the effect of the CO_2 absorption in the molecular structure of the ionic
236 liquid. Also, accessing the FITR spectrum over time allowed to monitor the absorption kinetics.
237 Gas streams were analysed online using an Agilent gas chromatograph (GC) 7890B, equipped
238 with a thermal conductivity detector (TCD). The GC carrier gas was helium and the samples were
239 analysed using an isothermal method with a PoraPlot U column connected to a Molesieve 5A
240 column, at 313 K. The TCD detector temperature was maintained at 473 K. Gas samples were
241 introduced into the GC using an automated VICI-Valco gas valve.

242 To evaluate the maximum capacity of the proposed system, the absorption of CO_2 was
243 performed with a pure CO_2 feed stream, without regenerating the ionic liquid solution.
244 Afterwards, 3 cycles of CO_2 absorption / IL regeneration were conducted aiming to access the
245 regeneration efficiency, from the limit situation where the IL solution was fully saturated. Finally,
246 aiming real conditions simulation, experiments with a gas mixture of 65 mol% N_2O, 5% CO_2,
247 27% O_2 and 3% N_2, either 100% humidified or dried, were performed to evaluate the CO_2 removal
248 efficiency, determine the separation factor, as well as determine the effect of water vapour in the
249 process efficiency. The absorption flux of CO_2 and the overall mass transfer coefficient were also
250 determined.

3.4. Evaluation of experimental mass transfer coefficients

The parameters obtained by running the experimental set-up, allow to calculate the overall mass transfer coefficient, K_{ov}, according to the following equation:

$$K_{ov} = \frac{Q_g \times (C_{CO2,in,g} - C_{CO2,out,g})}{A \times \Delta C_{CO2,g,lm}} \qquad (10)$$

where the Q_g is the gas flow rate ($m^3.s^{-1}$) from the gas phase to the liquid phase, $C_{CO2,in,g}$ and $C_{CO2,out,g}$ are the gas phase inlet and outlet CO_2 concentrations ($mol.m^{-3}$), A is the gas-liquid contact area (m^2) and $\Delta C_{CO2,g,lm}$ is the logarithmic mean driving force based on the gas phase concentrations ($mol.m^{-3}$), described as:

$$\Delta C_{CO2,lm} = \frac{(C_{CO2} - C^*_{CO2})_{g,in} - (C_{CO2} - C^*_{CO2})_{g,out}}{ln\left[\left(C_{CO2} - C^*_{CO2}\right)_{g,in} \Big/ \left(C_{CO2} - C^*_{CO2}\right)_{g,out}\right]} \qquad (11)$$

$C^*_{CO2,in}$ and $C^*_{CO2,out}$ are the equilibrium concentrations at the interface between the gas and liquid phases. Due to the fast chemical reaction, CO_2 concentration in the liquid phase is equal to 0, and $C^*_{CO2,g}$ is 0. Therefore, the equation is simplified as follows:

$$\Delta C_{CO2,lm} = \frac{C_{CO2,g,in} - C_{CO2,g,out}}{ln\left[C_{CO2,g,in} \Big/ C_{CO2,g,out}\right]} \qquad (12)$$

Moreover, to determine the process efficiency, a separation factor (SF) between CO_2 and N_2O was determined. Considering the ratio between the permeable species in the feed and the permeate side, *SF* was determined according to the following equation:

$$SF = \frac{n_{i,p} \Big/ n_{j,p}}{n_{i,f} \Big/ n_{j,f}} \qquad (13)$$

where, p and f are the permeate and feed streams and i and j the permeable species, in particular i the most permeable one.

4. Results and discussion

4.1. [Cho][Lys] characterization

In this work, due to the low toxicity and low production cost, when compared to other traditional ILs, and recognized efficiency to capture CO_2, [Cho][Lys] was the IL selected to absorb CO_2 using a membrane contactor system, aiming the operation in a closed-loop anaesthetic circuit. To increase the cost-effectiveness of this IL, it is proposed the use of an aqueous solution of [Cho][Lys]. As referred in section 3.3, a pre-screening study of CO_2 absorption with different [Cho][Lys] IL concentrations was performed. According to the results obtained, the highest CO_2 absorption was achieved for the IL solution with 60 wt% of [Cho][Lys] (Figure 3a). However, the solution must possess low viscosity to minimise the gas-liquid mass transfer resistance and increased pressure in the capillaries. Therefore, dynamic viscosities of the IL solutions were measured, as shown in Figure 3b. The viscosity obtained for the IL solution with 60 wt% of [Cho][Lys] was 36 mPa.s, at 293 K, while for the 50 wt% [Cho][Lys] was significantly lower (15 mPa.s). Since a slight difference in the CO_2 absorption between both IL solutions was obtained, 50 wt% [Cho][Lys] was the concentration selected to perform the present study. Additionally, in the case of the 50 wt% solution, the CO_2 absorption kinetics is faster when compared to the 60 wt% solution, which leads to a faster CO_2 removal rate, as it can be observed in Figure 3a, that presents the pressure profiles for the first hours of the experiments.

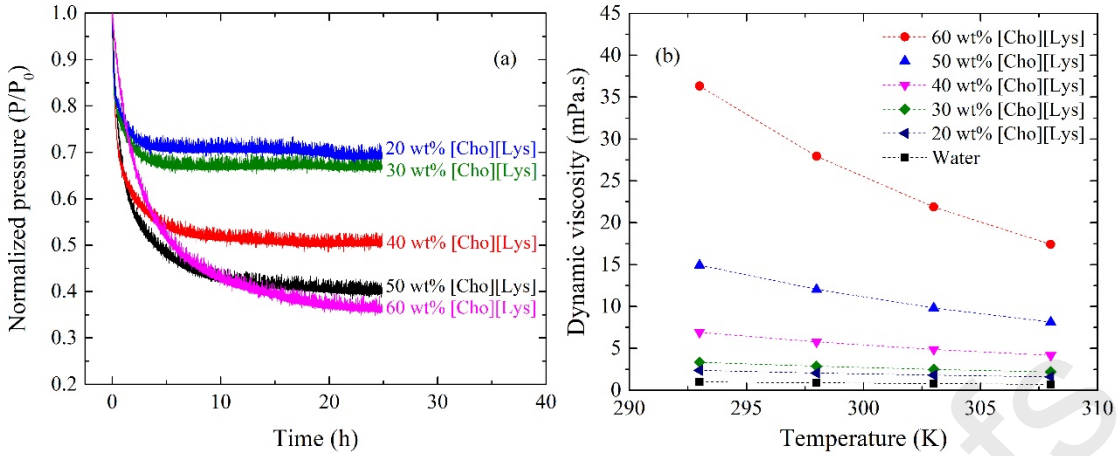

Figure 3. (a) Screening of CO_2 absorption in different [Cho][Lys] aqueous solutions; (b) Dynamic viscosity of different [Cho][Lys] aqueous solutions as a function of temperature.

The thermal stability of the CO_2 absorbents is extremely relevant and must be taken into account, as it can affect their absorption and desorption behaviour [15]. In a typical hospital surgery room temperature ranges between 293 and 297 K [34], and [Cho][Lys] is stable against temperature variations, as it is demonstrated in Figure 4. Furthermore, in a perspective of possible thermal regeneration, the temperatures should not go higher than 453 K, which corresponds to the onset temperature where weight loss was registered due to thermal degradation (Figure 4).

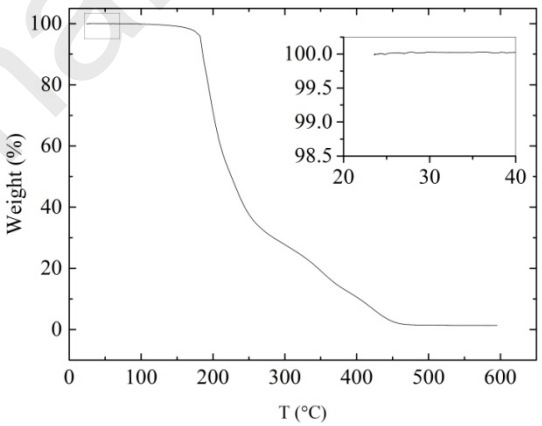

Figure 4. Thermogravimetric curve for [Cho][Lys] as a function of temperature.

The contact angle obtained between the 50 wt% [Cho][Lys] solution and the PTFE membrane was 97°, at 295 K. Contact angles higher than 90° are associated to hydrophobic surfaces and usually used as a reference to operate membrane modules in a non-wetted pore mode, avoiding

liquid penetration and stagnation inside the pores [35]. Therefore, the PTFE modules selected for this work assure that the pores of the membrane are not affected by wetting with the liquid phase. This is an important feature that allows the operation of the system without resistance to mass transfer due to the presence of the membrane.

4.2. CO_2 capture maximum absorption capacity

The absorption of CO_2 was performed using a pure CO_2 feed stream, to access the maximum absorption capacity of the [Cho][Lys] solution (50 wt%). The CO_2 flow rate was adjusted to 250 $mL.min^{-1}$, which is analogous to the minimal-flow anaesthesia mode [33]. The CO_2 absorption by the ionic liquid occurs across the gas-liquid interface, due to the contact between the stabilised phases inside the pores of the PTFE capillaries of the membrane contactor.

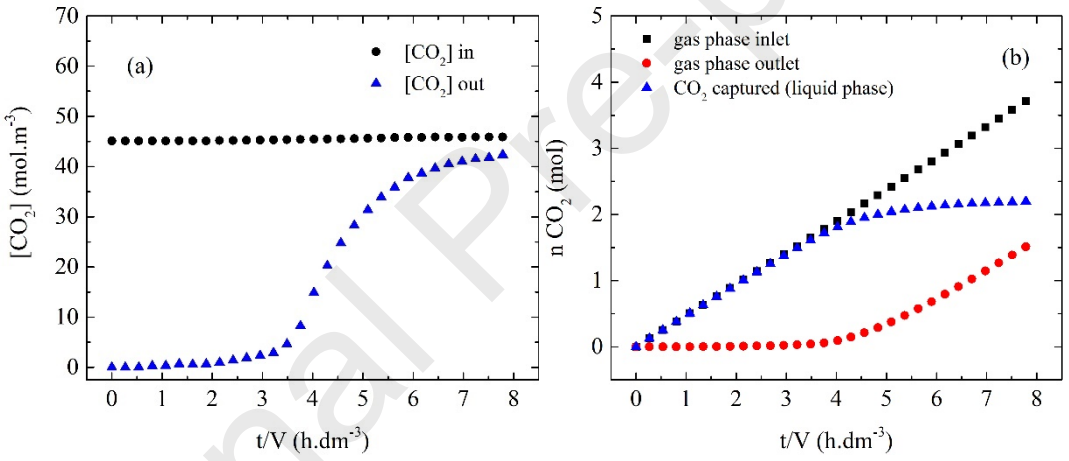

Figure 5. Experimental CO_2 absorption curves: (a) inlet and outlet [CO_2] in the gas phase as a function of time per IL solution volume; (b) Accumulated [CO_2] in gas and liquid phases as a function of time per IL solution volume.

In Figure 5a is represented the CO_2 concentration of the inlet and outlet streams in the gas phase as a function of time *per* volume of IL. Since the process is completely controlled by the liquid phase, the duration of the experiments is dependent of the volume of the IL solution used, thus in the present work, the time variable is always shown by the ratio time *per* IL volume used in each experiment. The profile obtained for the CO_2 concentration in the gas outlet stream is the result of an absorption accompanied by chemical reaction. Once the liquid phase approaches saturation, we started to observe the presence and increase of CO_2 concentration in the gas outlet stream. The number of CO_2 moles captured by the liquid phase was obtained assuming the difference between

the inlet and outlet streams in the gas phase, which is related with the CO_2 absorption by the IL (Figure 5b). The absorption of CO_2, in this case, was performed using 700 mL of 50 wt% [Cho][Lys] solution and a liquid flow rate of 524 $mL.min^{-1}$. Saturation was achieved after 5.5 hours of operation, corresponding to a time *per* IL volume of 7.8 $h.dm^{-3}$. According to equation (10), the overall mass transfer coefficient can be calculated through the ratio between the CO_2 absorption flux and the mean logarithmic CO_2 concentration in the gas phase (driving force). The value obtained for K_{ov} was 2.16×10^{-5} $m.s^{-1}$ with a CO_2 flux of 1.82×10^{-4} $mol.m^{-2}.s^{-1}$. The total amount of CO_2 captured was 5.9 mol_{CO2}/kg_{IL}, which is superior to the maximum absorption capacity of soda lime reported in literature (19 wt%, which corresponds to 4.32 mol/kg) [36].

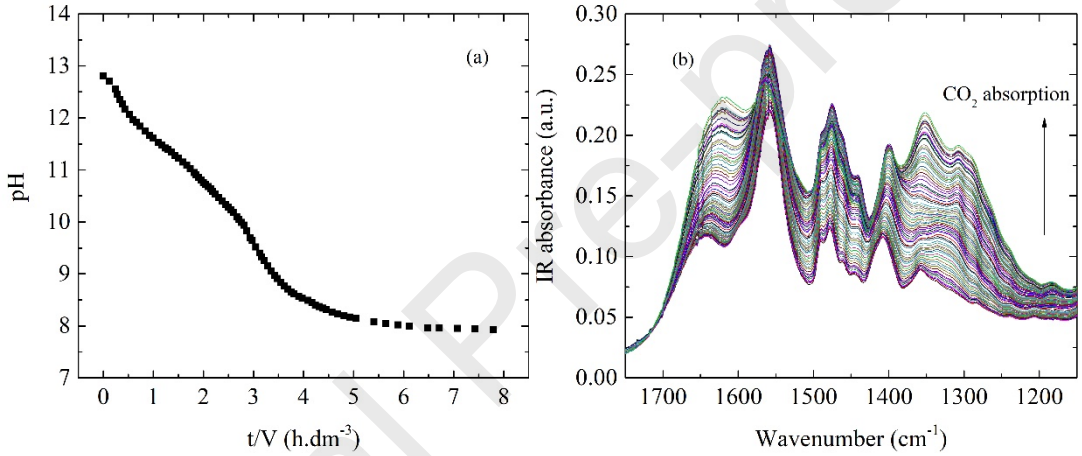

Figure 6. CO_2 absorption in [Cho][Lys] IL solution, monitored by pH measurement and ATR-FTIR analysis: (a) pH variation as a function of time per IL solution volume; (b) IR absorbance as a function of the wavenumber.

The absorption of CO_2 by the IL was followed by measuring the pH *in situ* and performing an IR spectra analysis of the IL samples. In Figure 6a, the pH variation during the CO_2 absorption is represented. [Cho][Lys] solution possess a strong basic character which is confirmed through the extremely high initial pH (~13). Due to this strong basicity, the IL is very reactive towards CO_2. The pH decreases over time as a consequence of the neutralization reaction between CO_2 and [Cho][Lys] solution due to the formation of the bicarbonate anion. The saturation state of the IL solution is represented by the plateau obtained at pH ~8. Figure 6b is a representation of the CO_2 absorption impact at a molecular level. Representative differences were obtained in the FTIR

spectra of the samples before and after CO_2 absorption, characterized by an increase of the absorbance bands at 1647 cm^{-1}, 1558 cm^{-1}, 1478 cm^{-1}, 1408 cm^{-1} and 1358 cm^{-1}. The absorbance band corresponding to the $-NH_3^+$ group is observed at the region 1600-1750 cm^{-1} [37]. Therefore, the band at 1647 cm^{-1} is attributed to the protonated amine groups, which formation was predicted by the chemical model as described in section 2.1. An absence of a band in the 2500-3000 cm^{-1} region after the CO_2 absorption, indicates no formation of carbamic acid. Generally, the interaction between amine groups and CO_2 can proceed through carbamate or carbamic acid formation pathways. Hence, the pathway of carbamic acid formation was not considered in the chemical mechanism described in the present work [28,37]. The two bands at 1558 cm^{-1} and 1408 cm^{-1} correspond to the asymmetric and symmetric stretching vibrations of COO^-, respectively. Depending on the molecular constituents, carboxylates bands are generally present in the 1650-1540 cm^{-1} and 1450-1360 cm^{-1} regions. Inorganic carbonates do not possess C-0 and C=0 stretching vibrations. Thus, the "C-O" bond order of the inorganic carbonates is between one and two, possessing a stretching vibration band in the region 1410-1510 cm^{-1}. The identified band at 1478 cm^{-1} is then attributed to the vibration of the carbonate ion CO_3^{2-} [38,39]. Therefore, the FTIR spectra analysis of the IL solution after CO_2 absorption confirmed the formation of the ionic species bicarbonate ion HCO_3^-, protonated amine NH_3^+ and carbonate ion CO_3^{2-}, as described by the proposed chemical mechanism (equations (1) to (5) in section 2.1).

Regarding to analytical methods, especially in cases of process monitoring, it is important to mention that both pH measurements and IR spectra analysis are fast techniques, clean and easy to use, which allow for an efficient monitoring of the CO_2 loading in the ionic liquid solution.

4.3. CO_2 maximum absorption capacity and IL solution regeneration cycles

Regeneration of the IL solution integrated with the CO_2 absorption can be a step forward when comparing to the current technology, since soda lime is disposed after reaching its saturation, adding an extra cost to the hospitals. In Figure 7 are represented the CO_2 maximum absorption and IL regeneration cycles, with the pH evolvement as a function of time *per* IL volume (a) and the CO_2 loading as a function of time per IL volume (b).

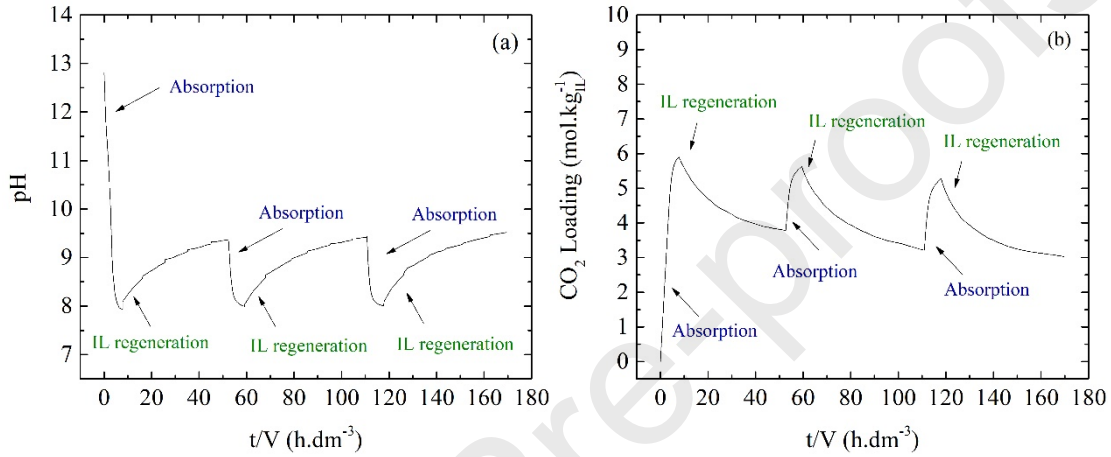

Figure 7. CO_2 absorption and IL regeneration cycles: (a) pH as a function of time per IL solution volume; (b) CO_2 loading as a function of time per IL solution volume.

Cycles of CO_2 absorption/IL regeneration were performed, where the CO_2 absorption was accomplished feeding as gas stream pure CO_2 and the IL regeneration with N_2 as the sweep gas. In the first cycle, the complete saturation of the IL was achieved, corresponding to a CO_2 loading value of 5.9 mol_{CO2}/kg_{IL}. The IL regeneration efficiency, after the saturation state was 36%, which corresponds to the disruption of the weaker chemical bond between the amine in the carboxylic acid functional group of the lysinate anion and bicarbonate. In the second cycle, the resulting CO_2 absorption capacity corresponded to what was reverted in the first regeneration cycle. In the second and third absorption/regeneration cycles, the regeneration was complete, since the amount of CO_2 absorbed in the previous absorption step was totally reverted, as it is demonstrated in Figure 7b. Therefore, if a complete regeneration is desired starting from the first cycle, that will probably be possible by performing a thermal regeneration step, in order to revert the remaining

389 bond between bicarbonate and the amine group in the alkyl side chain of lysinate anion and, by
390 this mean, exploit the full potential of the IL solution.

391 *4.4. CO_2 removal from anaesthetic gas mixtures*

392 In a closed-loop operation perspective, the content of CO_2 in the recirculated anaesthetic gas
393 mixture must be lower than 0.5%, to avoid hypercapnia (high levels of CO_2 in blood), hypoxemia
394 or hypoxia (low levels of O_2 in blood and tissue). The anaesthetic gas mixture to be recovered
395 contain around 5% of CO_2, thus, the following results correspond to experiments aiming an
396 operation efficiency superior to 90%.

397 To evaluate the CO_2 capture from anaesthetic gas mixtures, experiments considering
398 nitrous oxide as the anaesthetic gas were conducted, simulating realistic conditions. Therefore, a
399 gas mixture composition of 65% N_2O, 5% CO_2, 27% O_2 and 3% N_2 was used to feed the module,
400 mimicking the exhalation of a patient. In addition, experiments with 100% humidified feed gas
401 stream and with simultaneous IL regeneration were also performed. In Table 3 the experimental
402 and calculated mass transfer parameters obtained are shown.

403

404

405 *Table 3. Experimental and calculated mass transfer parameters.*

Parameters	***5% CO_2***	***5% CO_2 + 100% RH***	***5% CO_2 + 100% RH + IL regeneration***
u_l $(m.s^{-1})$	1.39		
k_l x 10^{-6} $(m.s^{-1})$	9.26		
Volume of.IL (dm^3)	0.75	0.80	1.35
Time *(h)*	36	39	63
Time/IL volume $(h.dm^{-3})$	47.7	48.5	46.9
J CO_2 x 10^{-6} $(mol.m^{-2}.s^{-1})$	8.34	8.55	8.46
J N_2O x 10^{-6} $(mol.m^{-2}.s^{-1})$	4.43	4.83	5.75
$K_{CO2,overall}$ x 10^{-6} $(m.s^{-1})$	9.15	9.36	9.33
φ	1.25	1.28	1.28
SF	21.4	18.6	14.6
CO_2 *Loading* $(mol.kg^{-1})$	3.14	2.92	2.86

406

407 The obtained flux of CO_2 was identical for all experiments, using N_2O in the gas mixture
408 as the anaesthetic gas. Therefore, the presence of water in the gas mixture and the simultaneous
409 IL regeneration do not compromise the CO_2 mass transfer. The regeneration step does not affect
410 the CO_2 transport, since the driving force was already the maximum possible, due to the fast
411 reaction between CO_2 and the liquid phase, resulting in an immediate consumption of CO_2. The

412 experimental time obtained for all cases, shown in Table 3, correspond to operation efficiency
413 above 90%, meaning a CO_2 content in the recycled gas mixtures lower than 0.5%, as required.
414 This experimental condition explains why the values obtained for the CO_2 loadings expressed in
415 Table 3 are inferior to the reported in section 4.3, since the CO_2 content of 0.5% in the recycled
416 gas stream is detected before the IL solution reaches its complete saturation.

417 When the feeding gas mixture was humidified, the presence of water vapour leads to an
418 increase of N_2O flux. The mass transport in the proposed system is controlled by the chemical
419 reaction between CO_2 and the IL solution, however the presence of water vapour in the gas phase
420 may lead to the formation of water microdomains in the ionic liquid phase, offering and additional
421 path for the transport of solutes through the ionic liquid phase. The increase of N_2O flux observed
422 may be justified by the solubility of N_2O in water and the mobility of these water
423 microenvironments across the liquid phase. A similar behaviour was already reported in the
424 literature [40,41].

425 Additionally, when the simultaneous IL solution regeneration step was added, the N_2O
426 flux increased. This behaviour results from the removal of N_2O during regeneration, keeping high
427 the driving force for transport during the absorption process. This additional transport path has
428 almost no impact on the transport of CO_2 because, due to its fast reaction at the gas-liquid
429 interface, its concentration in a free form inside the liquid phase is negligible. Still, the overall
430 selective removal of CO_2 from the gas phase, when compared with the transport of N_2O, is rather
431 impressive if we remember that these molecules possess similar properties, such as molecular
432 mass, chemical configuration, molecular volume, electronic structure and kinetic diameters
433 (Table 4), that explain their similar solubility and diffusivity in water.

434

435

436 *Table 4. Lennard-Jones and kinetic diameters.*

	Lennard-Jones diameter	Kinetic diameter

	(Å)	(Å)
CO_2	3.941 [30]	3.330 [42]
N_2O	3.828 [30]	3.330 [43]

Also, it is important to mention the very low partial pressure of CO_2 (5% mol) compared with the partial pressure of N_2O (65% mol) in the feed stream, and even though there was a transport of N_2O to the liquid phase, the removal of CO_2 was not affected. The separation factors obtained (*SF*), shown in Table 3, are considerable high for all cases, which is a proof that the proposed system is very selective towards CO_2. For the experimental procedure mimicking the real conditions, *i.e.*, containing 65% of the anaesthetic gas humidified, the system proposed with simultaneous IL regeneration, was able to operate efficiently during 63 hours.

In the current technology, that utilises containers with 1 kg of soda lime for CO_2 capture in anaesthetic closed circuits, it is recommended to replace the container after 8 to 14 hours of continuous operation, depending on the supplier recommendations and the usage. Furthermore, the maximum absorption capacity of soda lime to capture CO_2 is 4.32 mol/kg [36]. Based on the results obtained in this work, the proposed system was able to operate over 63 hours using 1.44 kg of 50 wt% [Cho][Lys] IL solution with a maximum absorption capacity of 5.9 mol/kg. Comparing with the use of a container with 1 kg of soda lime, the proposed system possesses a working operation time 3 to 5 times higher of 1 kg of [Cho][Lys] IL solution is used (~43 hours of operation).

5. Conclusions

Experiments of CO_2 capture from gas mixture with anaesthetic agents, have been performed, using a 50 wt% [Cho][Lys] IL solution. The system was composed by polytetrafluoroethylene porous membrane contactors with the IL solution circulating in counter current with the gas phase in the lumen of the capillaries. Additionally, a regeneration unit composed by a second membrane contactor was simultaneously operated. The results obtained revealed a CO_2 capture maximum

460 capacity of the system of 5.9 mol/kg_{IL}. In the experiments in which simulated conditions using
461 65% of nitrous oxide and 5% of carbon dioxide, the results revealed an efficient system able to
462 operate over 63 hours. However, the regeneration of the IL solution using N_2 as sweep gas, was
463 not completely efficient for the reversion of the CO_2 absorption. Due to this fact, a thermal
464 regeneration study is recommended as future work. Additionally, the proposed system should be
465 tested using a feed stream mimicking real conditions, using the exhaled composition as well as
466 with pulsed flow, simulating the expiratory frequency.

467 ***Acknowledgements***

468 This work was supported by the Associate Laboratory for Green Chemistry - LAQV - which is
469 financed by national founds from FCT/MCTES (UID/QUI/50006/2019). C. F. Martins
470 acknowledge Fundação para a Ciência e Tecnologia (FCT) for the fellowship
471 SFRH/BD/111128/2015. Luísa Neves acknowledge FCT for her exploratory project grant
472 IF/00505/2014/CP1224/CT0004 attributed within the 2014 FCT research program.

473

6. References

[1] W. Funk, M. Gruber, K. Wild, J. Hobbhahn, Dry soda lime markedly degrades sevoflurane during simulated inhalation induction, Br. J. Anaesth. 82 (1999) 193–198.

[2] I. Lund, L.L. Andersen, H. Erikson, Efficiency of carbon dioxide absorption by soda lime in a closed system, Br. J. Anaesth. 28 (1956) 13–19.

[3] S. Lagorsse, F.D. Magalhães, A. Mendes, Xenon recycling in an anaesthetic closed-system using carbon molecular sieve membranes, J. Memb. Sci. 301 (2007) 29–38.

[4] A.F. Portugal, F.D. Magalhães, A. Mendes, Carbon dioxide removal from anaesthetic gas circuits using hollow fiber membrane contactors with amino acid salt solutions, J. Memb. Sci. 339 (2009) 275–286.

[5] D.K. Spracklin, E.D. Kharasch, Evidence for metabolism of fluoromethyl 2,2-difluoro-1-(trifluoromethyl)vinyl ether (compound A), a sevoflurane degradation product, by cysteine conjugate β-lyase, Chem. Res. Toxicol. 9 (1996) 696–702.

[6] H. Wissing, D. Ph, I. Kuhn, U. Warnken, D. Ph, R. Dudziak, D. Ph, Carbon monoxide production from Desflurane , Enflurane , Halothane , Isoflurane , and Sevoflurane with dry soda lime, Anesthesiology. 95 (2001) 1205–1212.

[7] H. Bito, Y. Ikeuchi, K. Ikeda, Effects of the water content of soda lime on Compound A concentration in the anesthesia circuit in sevoflurane anesthesia, Anesthesiology. 88 (1998) 66–71.

[8] G.T. Rochelle, Amine Scrubbing for CO_2 Capture, Science. 325 (2009) 1652–1654.

[9] R.R. Bottoms, Process for separating acidic gases, US Pat. 1783901. (1930).

[10] N.M. Simon, M. Zanatta, F.P. Santos, M.C. Corvo, J. Eurico, N.M. Simon, M. Zanatta, P. Santos, M.C. Corvo, J. Eurico, J. Dupont, Carbon dioxide capture by aqueous ionic liquid solutions, ChemSusChem. 10 (2017) 4927–4933.

[11] J. Ma, Z. Zhou, F. Zhang, C. Fang, Y. Wu, Z. Zhang, A. Li, Ditetraalkylammonium Amino Acid Ionic Liquids as CO_2 Absorbents of High Capacity, Environ. Sci. Technol. 45 (2011) 10627–10633.

[12] Z. Zhijun, D. Haifeng, Z. Xiangping, The Research Progress of CO_2 Capture with Ionic Liquids, Chinese J. Chem. Eng. 20 (2012) 120–129.

[13] S.D. Kenarsari, D. Yang, G. Jiang, S. Zhang, J. Wang, A.G. Russell, Q. Wei, M. Fan, Review of recent advances in carbon dioxide separation and capture, RSC Adv. 3 (2013) 22739–22773.

[14] O. Cabeza, Chapter 1 - Properties and Green Aspects of Ionic Liquids, Elsevier, 2014.

[15] B. Li, Y. Chen, Z. Yang, X. Ji, X. Lu, Thermodynamic study on carbon dioxide absorption in aqueous solutions of choline-based amino acid ionic liquids, Sep. Purif. Technol. 341 (2019) 128–138.

[16] Q. Yang, Z. Wang, Z. Bao, Z. Zhang, Y. Yang, Q. Ren, New Insights into CO_2 Absorption Mechanisms with Amino-Acid Ionic Liquids, ChemSusChem. 9 (2016) 806–812.

[17] S. Bhattacharyya, F.U. Shah, Ether functionalized choline tethered amino acid ionic liquids for enhanced CO_2 capture, ACS Sustain. Chem. Eng. 4 (2016) 5441–5449.

[18] S. Saravanamurugan, A.J. Kunov-kruse, R. Fehrmann, A. Riisager, Amine-functionalized amino acid-based ionic liquids as efficient and high-capacity absorbents for CO_2, ChemSusChem. 7 (2014) 897–902.

[19] C.F. Martins, L.A. Neves, M. Estevão, A. Rosatella, V.D. Alves, C.A.M. Afonso, J.G. Crespo, I.M. Coelhoso, Effect of water activity on carbon dioxide transport in cholinium-based ionic liquids with carbonic anhydrase, Sep. Purif. Technol. 168 (2016) 74–82.

[20] P.S. Kumar, J.A. Hogendoorn, P.H.M. Feron, G.F. Versteeg, New absorption liquids for

the removal of CO_2 from dilute gas streams using membrane contactors, Chem. Eng. Sci. 57 (2002) 1639–1651.

[21] B. Chen, J. Li, B. Chen, Review of CO2 absorption using chemical solvents in hollow fiber membrane contactors, Sep. Purif. Technol. 41 (2005) 109–122.

[22] J. Albo, P. Luis, A. Irabien, Absorption of coal combustion flue gases in ionic liquids using different membrane contactors, Desalin. Water Treat. 27 (2011) 54–59.

[23] Z. Dai, L. Ansaloni, L. Deng, Precombustion CO_2 capture in polymeric hollow fiber membrane contactors using ionic liquids : porous membrane versus nonporous composite membrane, Ind. Eng. Chem. Res. 55 (2016) 5983–5992.

[24] R. Wang, H.Y. Zhang, P.H.M. Feron, D.T. Liang, Influence of membrane wetting on CO_2 capture in microporous hollow fiber membrane contactors, Sep. Purif. Technol. 46 (2005) 33–40.

[25] G. Obuskovic, K.K. Sirkar, Liquid membrane-based CO_2 reduction in a breathing apparatus, J. Memb. Sci. 389 (2012) 424–434.

[26] M. Malankowska, C.F. Martins, H.S. Rho, L.A. Neves, R.M. Tiggelaar, J.G. Crespo, M.P. Pina, R. Mallada, H. Gardeniers, I.M. Coelhoso, Microfluidic devices as gas – Ionic liquid membrane contactors for CO_2 removal from anaesthesia gases, J. Memb. Sci. 545 (2018) 107–115.

[27] E. Chabanon, E. Kimball, E. Favre, O. Lorain, E. Goetheer, D. Ferre, A. Gomez, P. Broutin, Hollow Fiber Membrane Contactors for Post-Combustion CO_2 Capture : A Scale-Up Study from Laboratory to Pilot Plant, 69 (2014) 1035–1045.

[28] J. Sun, N.V.S.N.M. Konda, J. Shi, R. Parthasarathi, T. Dutta, F. Xu, C.D. Scown, A. Simmons, S. Singh, CO_2 enabled process integration for the production of cellulosic ethanol using bionic liquids, Energy Environ. Sci. 9 (2016) 2822–2834.

[29] B.W. Reed, M.J. Semmens, E.L. Cussler, Chapter 10 - Membrane contactors, Volume 2,

548 Elsevier, 1995.

549 [30] E.L. Cussler, Diffusion - Mass transfer in fluid systems, 3rd Ed., Cambridge Series in
550 Chemical Engineering. Cambridge University Press., 2009.

551 [31] L.A. Neves, C. Afonso, I.M. Coelhoso, J.G. Crespo, Integrated CO_2 capture and
552 enzymatic bioconversion in supported ionic liquid membranes, Sep. Purif. Technol. 97
553 (2012) 34–41.

554 [32] M.R. Nel, J.D. Watts, G.G. Lockwood, An alternative method of nitrous oxide delivery
555 into a minimal-flow circle breathing system, Anaesthesia. 52 (1997) 57–61.

556 [33] G. Mychaskiw, Low and minimal flow anesthesia: Angels dancing on the point of a
557 needle, J. Anaesthesiol. Clin. Pharmacol. 28 (2012) 423.

558 [34] P.H. Langowski, A.K. Seth, T. Cohen, D.E. Shaughnessy, G.A. Freeman, M.P. Sheerin,
559 R.J. Weber, G.L. Hendrickson, M.R. Keen, M.E. Woolsey, H.F. Crowther, J.A. Kohler,
560 C.E. Marriott, R.M. Martin, S.T. Bushby, F. Myers, K.W. Cooper,
561 ANSI/ASHRAE/ASHE standard 170-2013 - Ventilation of health care facilities., in:
562 American Society of Heating, Refrigerating and Air-Conditioning Engineers, Inc.,
563 Atlanta, 2008.

564 [35] Y. Yuan, T.R. Lee, Chapter 1 - Contact Angle and Wetting Properties, Springer, 2013.

565 [36] B.S. Freeman, Chapter 17 - Absorption of Carbon Dioxide, in: Anesthesiol. Core Rev.
566 Part One Basic Exam, McGraw-Hill Education, 2014.

567 [37] Y. Sistla, A. Khanna, CO_2 absorption studies in amino acid-anion based ionic liquids,
568 Chem. Eng. J. 273 (2015) 268–276.

569 [38] K. Robinson, A. Mccluskey, M.I. Attalla, An FTIR Spectroscopic Study on the Effect of
570 Molecular Structural Variations on the CO_2 Absorption Characteristics of Heterocyclic
571 Amines, ChemPhysChem. 12 (2011) 1088–1099.

572 [39] B. Smith, Infrared Spectral Interpretation: A systematic approach, CRC press, New

York, 1999.

[40] R. Fortunato, M.J. González-Muñoz, M. Kubasiewicz, S. Luque, J.R. Alvarez, C.A.M. Afonso, I.M. Coelhoso, J.G. Crespo, Liquid membranes using ionic liquids: The influence of water on solute transport, J. Memb. Sci. 249 (2005) 153–162.

[41] J. Wang, J. Luo, S. Feng, H. Li, Y. Wan, X. Zhang, Recent development of ionic liquid membranes, Green Energy Environ. 1 (2016) 43–61.

[42] A.F. Ismail, K.C. Khulbe, T. Matsuura, Gas separation membranes: Polymeric and inorganic, 2015.

[43] S. Matteucci, Y. Yampolskii, B.D. Freeman, I. Pinnau, Transport of Gases and Vapors in Glassy and Rubbery Polymers, 2006.